PAPER

Check for updates

Novel dual-site fluorescent probe for monitoring cysteine and sulfite in living cells†

Xin Guo,‡[a] Lili Xia,‡[b] Jinxin Huang,[b] Yiming Wang,[a] Yueqing Gu*[b] and Peng Wang [ID] *[b]

Fluorescent probes have been considered to be efficient tools for the visualization of physiological and pathological processes. Herein, a dual-site fluorescence probe denoted as **LC-1** was developed for the detection of cysteine (Cys) and its metabolite SO_3^{2-}. The probe was shown to be highly sensitive to Cys and SO_3^{2-} with a turn-on mode fluorescence signal through two emission channels under excitations at wavelengths of 320 nm and 440 nm. Notably, the **LC-1** probe was also observed to be satisfactorily sensitive to Cys and SO_3^{2-} in the presence of other amino acids and reactive oxygen species (ROS). Meanwhile, **LC-1** was shown to have low cytotoxicity and was successfully applied for imaging the metabolism of Cys in living cells.

1. Introduction

Cysteine (Cys), a small-molecule sulfhydryl-containing amino acid, plays crucial roles in intracellular signal transduction and maintaining redox homeostasis in the biological environment.[1–3] Sulfur dioxide (SO_2) can be endogenously produced by oxidation of sulfhydryl-containing amino acids like Cys by utilizing specific enzymes. Cysteine dioxygenase has been shown to catalyze the conversion of cysteine to cysteinesulfinate, which is a substrate of aspartate aminotransferase. The converted β-sulfinylpyruvate decomposes to pyruvate and SO_2 in mammals. These two substances exist as aqueous sulfites (HSO_3^{2-} and SO_3^{2-}) when used in biological processes.[4–7] Cys is normally present in the human body at concentrations between about 30 and 200 μM, and acts as an extracellular reducing agent and substrate for protein synthesis as well as a precursor of (glutathione) GSH. A deficiency or excess amount of Cys is implicated in edema, liver damage, skin lesions, Parkinson's disease, Alzheimer's disease and other pathological conditions.[8–11] Thus achieving the normal equilibrium concentration of Cys is of great importance for many physiological processes.

The use of fluorescent probes has become popular because of their noninvasiveness, high sensitivity and real-time detection.[12–16] Various fluorescent probes have been designed and reported for the detection of Cys *in vitro* and *in vivo*, and have been used to simultaneously distinguish cysteine/ homocysteine, glutathione, and hydrogen sulfide in living cells,[17–25] and ratiometric fluorescent probes have been used to quantify cysteine.[26–30] Our group previously designed and synthesized several fluorescent probes for sensitively and selectively detecting Cys over other biothiols in living cells and mice.[31–33]

However, few of these reported probes could visualize the metabolic processes involving Cys.[34] Based on the reports of others and our previous work, we selected α,β-unsaturated acetonaphthone as the fluorophore and the thiol reaction site. And the benzaldehyde moiety was employed as the sensitive reaction site for SO_3^{2-} through nucleophilic addition. Finally, a dual-site probe, denoted as **LC-1**, for the detection of Cys and its metabolite SO_3^{2-} was rationally designed and synthesized. As expected, it exhibited high selectively and a rapid response to thiols and sulfite through two emission channels. The probe displayed satisfactory sensitivity towards Cys and sulfite with limits of detection of 1.5×10^{-7} M and 4.3×10^{-7} M, respectively. Moreover, cell imaging studies revealed the potential of using **LC-1** to monitor Cys and its metabolite SO_3^{2-} in living cells.

2. Experimental

2.1 General

All solvents and other reagents were of commercial quality and used without further purification. Absorption spectra were recorded using a microspectrophotometer (One drop, Nanjing, China). A PerkinElmer LS55 apparatus was utilized for acquiring fluorescence spectra. Laser confocal fluorescence microscopy (FluoView™, FV1000, Olympus, Japan) was employed for cell imaging. ^{1}H-NMR and ^{13}C-NMR spectra were acquired using a Bruker Advance 300-MHz spectrometer, with

[a] *Jiangsu Provincial Key Laboratory for Interventional Medical Devices, Huaiyin Institute of Technology, Huaian, Jiangsu Province, 223003, China*

[b] *Department of Biomedical Engineering, School of Engineering, China Pharmaceutical University, Nanjing 210009, China. E-mail: wangpeng159seu@hotmail.com*

‡ X. Guo and L. Xia contributed equally.

δ values in ppm relative to TMS. Mass data (ESI†) were acquired by performing quadrupole mass spectrometry.

2.2 Synthesis of LC-1

2-Acetyl-6-methoxynaphthalene (2 mmol, 0.4 g) and terephthalaldehyde (3 mmol, 0.402 g) were dissolved in ethanol (20 mL). Then piperidine (200 μL) was added to this solution, and the resulting mixture was refluxed for 48 hours. The refluxed mixture was cooled to room temperature, and then filtrated and washed with EtOH to obtain the crude product. The crude solid was purified by column chromatography to give the desired yellow solid **LC-1** in 65% yield. ^{1}H-NMR (300 MHz, DMSO-$d6$): δ 10.12 (s, 1H), 8.95 (s, 1H), 8.32 (d, J = 15.6 Hz, 1H), 8.11–8.21 (m, 4H), 7.96–8.01 (m, 3H), 7.89 (d, J = 15.7 Hz, 1H), 7.49 (d, J = 2.5 Hz, 1H), 7.35 (dd, J = 8.9, 2.5 Hz, 1H), 3.99 (s, 3H). ^{13}C-NMR (75 MHz, DMSO-$d6$): δ 192.5, 188.3, 159.6, 141.7, 140.4, 137.0, 136.9, 132.5, 131.3, 130.6, 129.8, 129.5, 129.3, 127.5, 127.3, 125.0, 124.7, 119.5, 106.2, 55.4. ESI-MS: 339.1 [M + Na]$^+$.

2.3 General fluorescence spectra measurements

All of the detection experiments were conducted in PBS buffer–DMSO (1 : 1, v/v). Analyte sample was added into a PBS buffer–DMSO (1 : 1, v/v) solution containing 20 μM of the **LC-1** probe, and the fluorescent intensity was monitored by using a fluorescence spectrometer.

2.4 Cell culture and confocal fluorescence imaging

The human breast adenocarcinoma cell line MCF-7 was purchased from American Type Culture Collection (ATCC; Manassas, VA, USA). Cells were cultured in DMEM (Invitrogen) supplemented with 10% fetal bovine serum (FBS, Hyclone), 100 μg mL^{-1} penicillin and 100 μg mL^{-1} streptomycin at 37 °C in a humidified atmosphere containing 5% CO$_2$. One day before imaging, cells were seeded in laser scanning confocal microscope (LSCM) culture dishes at a density of 5×10^5 cells per well. The dishes were subsequently incubated at 37 °C in a humidified atmosphere containing 5% CO$_2$. The control experiment involved incubating the cells with only 20 μM **LC-1** for 20 min. (For this control, **LC-1** was first dissolved in DMSO, and then the DMSO solution was added it into the cell culture medium; the concentration of DMSO was less than 0.5% in the cell culture medium.) For imaging SO$_3$$^{2-}$ in living cells, the cells were incubated with SO$_3$$^{2-}$ (1 mM) for 20 min, and then treated with **LC-1** for 20 min. For the thiol-blocking experiment, the cells were incubated with N-ethylmaleimide (NEM, 2 mM) for 60 min, and then co-incubated with **LC-1** for 20 min. For studying the metabolism of Cys in living cells, the cells are

incubated with N-ethylmaleimide (NEM, 2 mM) for 60 min, then co-incubated with Cys for 20 min, and finally incubated with **LC-1** for 180 min. The cells were washed three times with Dulbecco's PBS (pH 7.0) to remove free compound before analysis. Confocal luminescence images of MCF-7 cells were acquired using an Olympus FV1000 laser scanning confocal microscope.

2.5 Cytotoxicity assay

MCF-7 cells were seeded in a 96-well plate (1×10^4 cells per well). After cultivation for 24 h, **LC-1** at different concentrations were added to the wells ($n = 6$) and incubated for 24 h. (here, DMSO was dissolved first, and then the DMSO solution was added into the cell culture medium). Then a stock solution of MTT (20 μL; 5 mg mL^{-1}) was added to each well. After 4 h incubation at 37 °C, the MTT solution was replaced with 150 μL DMSO in each well. The absorbance in each well was measured at a wavelength of 570 nm with a multi-well plate reader. Cell viability was calculated using the formula cell viability = 100% × (mean absorbance of test wells − mean absorbance of medium control wells)/(mean absorbance of untreated wells − mean absorbance of medium control well).

3. Results and discussion
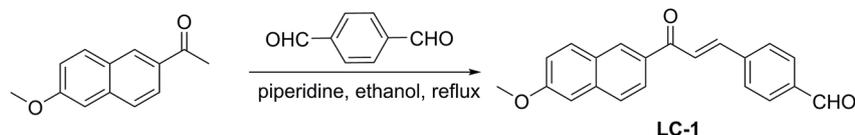
3.1 Synthesis of the LC-1 probe

The synthetic route to the **LC-1** probe is shown in Scheme 1. The commercial compound 2-acetyl-6-methoxynaphthalene was reacted with terephthalaldehyde under reflux in the presence of piperidine to give the desired **LC-1**. The chemical structure of **LC-1** was characterized by using ^{1}H NMR, ^{13}C NMR, and mass spectrometry.

3.2 UV-vis spectral properties of LC-1

We determined the UV-Vis spectral properties of the **LC-1** probe (20 μM) in PBS/DMSO (1/1, v/v, pH 7.4). **LC-1** displayed a wide absorption peak at about 320 nm (Fig. 1). Addition of Cys to **LC-1** yielded an obviously different UV-Vis spectrum: the maximum absorption peak decreased markedly in intensity and showed a hypochromatic shift to 315 nm. In contrast, upon the introduction of SO$_3$$^{2-}$, the maximum absorption peak of **LC-1** exhibited a bathochromic shift to 325 nm.

3.3 Spectral response of LC-1 to different concentrations of Cys

The response of the **LC-1** probe to different concentrations of Cys was investigated (Fig. 2). **LC-1** displayed almost no fluorescence emission under excitation at 320 nm in PBS/DMSO (1/1, v/v, pH 7.4). As the concentration of Cys was increased from
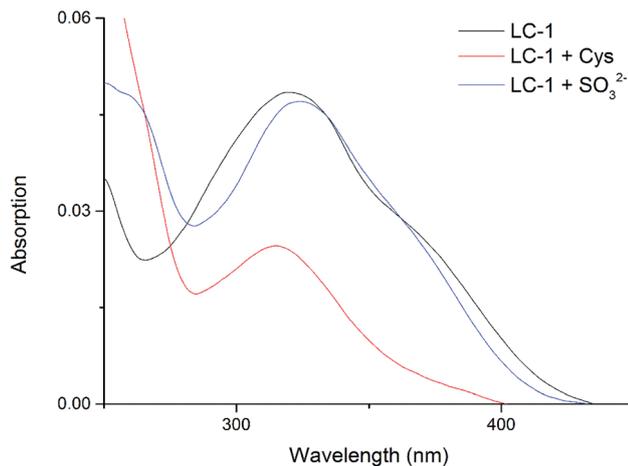

Scheme 1 Synthetic route to the **LC-1** probe.

Fig. 1 UV-vis absorption spectra of 20 μM **LC-1**, 20 μM **LC-1** with 400 μM Cys, and 20 μM **LC-1** with 400 μM SO_3^{2-}, each in a pH 7.4 aqueous 20 mM PBS buffer solution containing 50% DMSO.

0 to 400 μM, the fluorescence intensity of **LC-1** at 440 nm increased 150-fold. Moreover, the fluorescence intensity at this wavelength (I_{440nm}) showed a highly linear relationship with the concentration of Cys for Cys concentrations between 0 and 300 μM (r = 0.9933). The limit of detection (LOD) for Cys was calculated to be 1.5×10^{-7} M. The detection limit was calculated to be equal to $3\sigma/k$, where σ is the standard deviation of a blank measurement and k is the slope of the plot of the fluorescence intensity at 440 nm *versus* the concentration of Cys. This result suggested that our probe **LC-1** could be used to conduct a rapid quantitative analysis of Cys.

3.4 Spectral response of LC-1 to different concentrations of SO_3^{2-}

The capability of the **LC-1** probe to monitor SO_3^{2-} was also studied (Fig. 3). To detect sulfite, different concentrations of

Na_2SO_3 were added into respective samples of a solution of **LC-1** in PBS/DMSO (1/1, v/v, pH 7.4). Similar to the detection of Cys, the addition of Na_2SO_3 induced a distinct fluorescence emission at a wavelength of 530 nm under excitation at 440 nm. And a gradual increase in fluorescence intensity at 530 nm (I_{530nm}) was observed as the concentration of the sulfite was increased. Moreover, the fluorescence intensity at this wavelength (I_{530nm}) showed a highly linear relationship with the concentration of SO_3^{2-} for SO_3^{2-} concentrations between 0 and 200 μM, with a linear coefficient of 0.9906. According to the previous method, the limit of detection (LOD) of SO_3^{2-} was calculated to be 4.3×10^{-7} M. These results suggested that two emission channels of **LC-1** could be used to distinguish Cys from SO_3^{2-} and to determine their concentrations.

3.5 Response time and effect of pH

Then time-dependent changes of the fluorescence intensity of the **LC-1** probe in the presence of Cys or SO_3^{2-} were evaluated (Fig. S1†). The reaction between **LC-1** and Cys reached equilibrium within 5 min, while the detection of SO_3^{2-} by **LC-1** reached a plateau essentially instantly when monitoring the fluorescence at 530 nm. This difference showed that **LC-1** can be used to rapidly detect Cys and its decomposition product SO_3^{2-} and to identify which of these species is being detected.

To investigate the effects of pH on the fluorescence response of **LC-1** to Cys and SO_3^{2-}, the changes in the fluorescence of **LC-1** induced by Cys and SO_3^{2-} were each measured from pH 3 to 11 (Fig. S2†). The fluorescence intensity of **LC-1** at a wavelength of 440 nm was low. After the addition of Cys, the emission at 440 nm increased dramatically for the pH range 6–8. When SO_3^{2-} was added instead, the fluorescence intensity at 530 nm was strong for the pH range 4–8. These results revealed **LC-1** to be generally suitable for detecting Cys and SO_3^{2-} in physiological conditions.
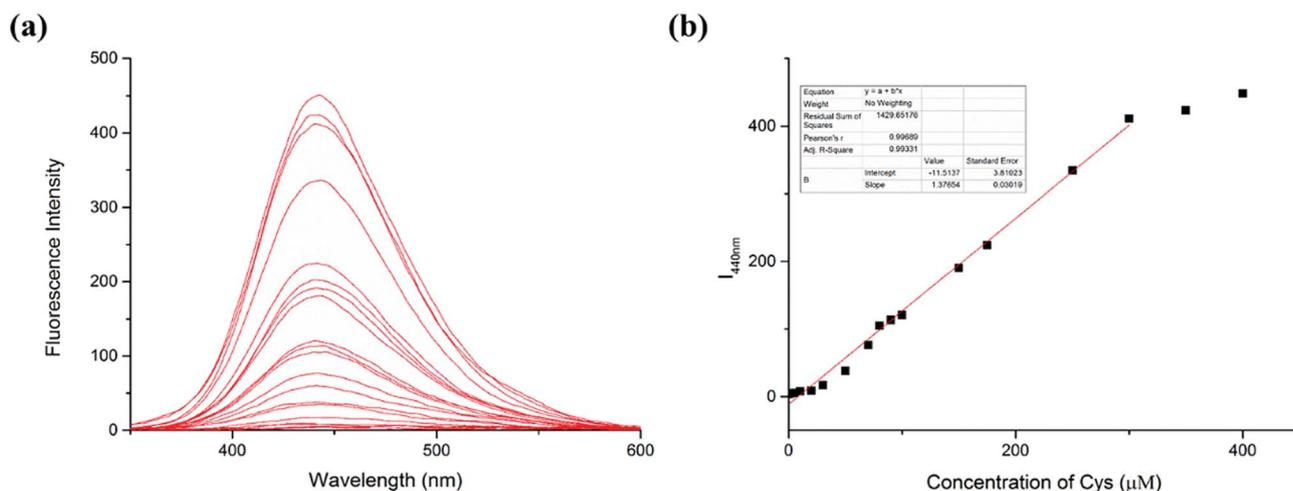

Fig. 2 (a) Fluorescence response of the **LC-1** probe (20 μM) to various concentrations (0–400 μM) of Cys, each in an aqueous solution (pH 7.4, 20 mM PBS buffer solution containing 50% DMSO). (b) Plot of I_{440nm} *versus* the concentration of Cys. Inspection of this plot revealed a linear relationship for Cys concentrations between 0 and 300 μM.
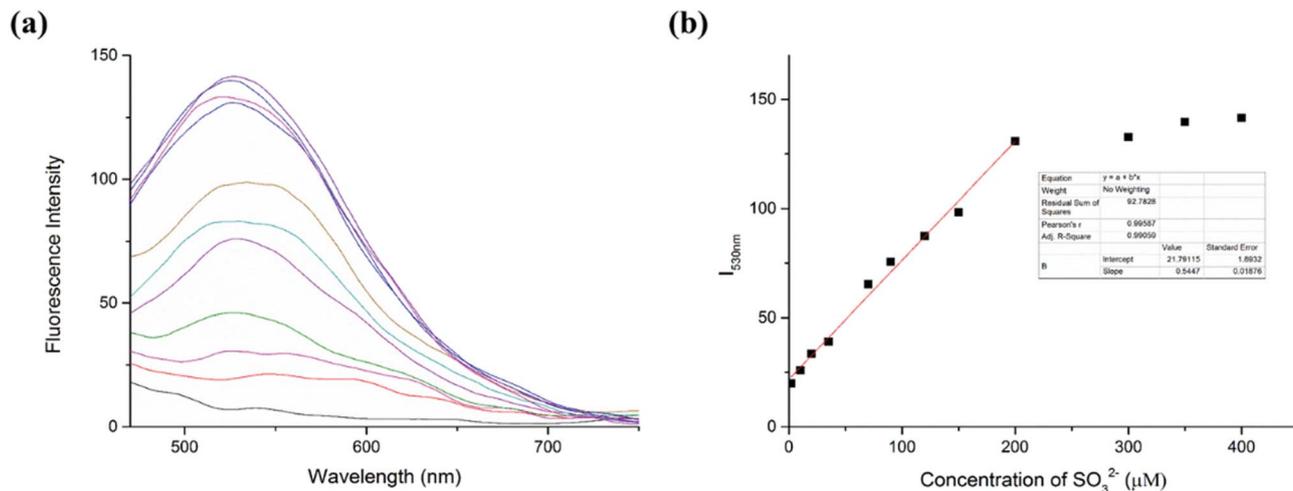
Fig. 3 (a) Fluorescence response of the **LC-1** probe (20 µM) to various concentrations (0–400 µM) of Na$_2$SO$_3$, each in an aqueous solution (pH 7.4, 20 mM PBS buffer solution containing 50% DMSO). (b) Plot of I_{530nm} *versus* the concentration of SO$_3^{2-}$. Inspection of this plot revealed a linear relationship for SO$_3^{2-}$ concentrations between 0 and 200 µM.

3.6 Selectivity experiments

To further demonstrate the selectivity of the **LC-1** probe toward different analytes, the fluorescence spectra were recorded in the presence of various amino acids and reactive oxygen species (ROS) under simulated physiological conditions (Fig. 4). Only Cys resulted in an obvious emission peak when excited at 320 nm while SO$_3^{2-}$ induced an intense fluorescence when a 440 nm excitation wavelength was used. These results showed the excellent selectivity of **LC-1** towards Cys and SO$_3^{2-}$ over other species.

3.7 Study of reaction mechanism

Based on our previous findings and other reports,[31,34] a mechanism for the response of the **LC-1** probe to Cys and SO$_3^{2-}$ was derived, and is shown in Scheme 2. The mechanism of the

response of **LC-1** to Cys was proposed to be based on the nucleophilic addition of the thiol in Cys to the α,β-unsaturated ketone in **LC-1** to form a thioether exhibiting blue fluorescence under excitation at 320 nm. The MS data for the Cys-**LC-1** system demonstrated this sensing mechanism (Fig. S3†). For the Na$_2$SO$_3$ detection system, the fluorescence change was proposed to be due to the addition of SO$_3^{2-}$ to the aldehyde group of **LC-1** leading to the turning on of green fluorescence. This sensing mechanism of the SO$_3^{2-}$-**LC-1** system was supported by the MS data, which showed a mass-to-charge (m/z) peak of 397.

3.8 Toxicity of LC-1 to cells

The cytotoxicity of the **LC-1** probe, specifically to MCF-7 cells, was assessed by carrying out the standard MTT assay (Fig. S4†).
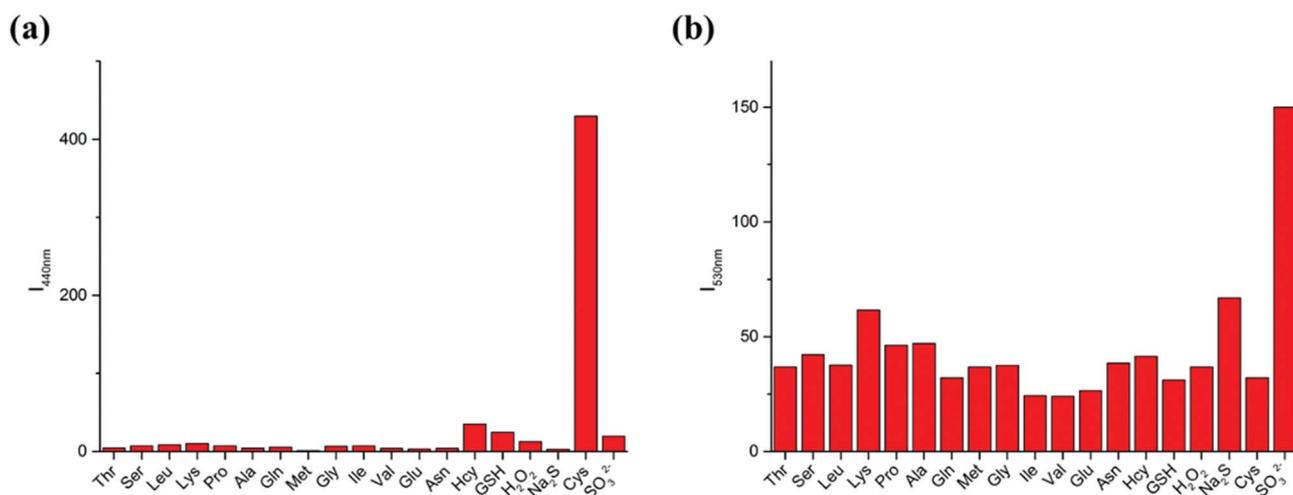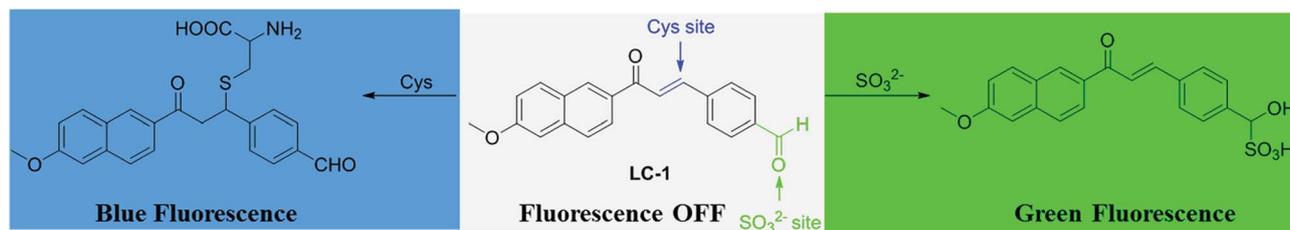

Fig. 4 Fluorescence responses of the **LC-1** probe (20 µM) to various relevant species (400 µM Thr, Ser, Leu, Pro, Ala, Gln, Met, Gly, Ile, Val, Glu, Asn, H$_2$O$_2$, Na$_2$S, Na$_2$SO$_3$, GSH, Cys and 10 µM Hcy), each in an aqueous solution (pH 7.4, 20 mM PBS buffer solution containing 50% DMSO). λ_{ex} = 320 nm (a) and 440 nm (b).

Scheme 2 Proposal for the mechanism used by the **LC-1** probe to detect Cys and SO_3^{2-}.

The cell viability was still over 85% after incubation even with a high 50 μM concentration of **LC-1**, indicating the good biocompatibility of **LC-1** with cells.

3.9 Fluorescence imaging in living cells

The applicability of the **LC-1** probe for cellular imaging was then assessed by using a confocal fluorescence microscope to simultaneously investigate whether **LC-1** can selectively detect Cys and SO_3^{2-} in living cells. As shown in Fig. 5 and 6, bright-field measurements confirmed the viability of the cells in the experimental environment. Cells whose thiols were scavenged by NEM (a well-known thiol-blocking reagent that was used to decrease the concentration of Cys in the control experiments) showed almost no fluorescence signals in both the blue and green channels when incubated with **LC-1** directly (Fig. 5b and 6b). The cells treated only with the **LC-1** probe exhibited strong fluorescence signals in the blue channel, owing to the endogenous Cys in living cells (Fig. 5e). And weak green fluorescence

from endogenous sulfite was also observed (Fig. 6e). When MCF-7 cells were incubated with the probe and SO_3^{2-}, a strong fluorescence emission was observed in the green channel (Fig. 6h). The present experiment provided additional evidence for the ability to use **LC-1** to selectively image Cys and SO_3^{2-} through two emission channels.

A long-duration imaging of Cys-loaded MCF-7 cells was also performed to monitor the metabolism of Cys in living cells (Fig. 7). After the cells were treated with NEM (2 mM), Cys (100 μM), and **LC-1** (10 μM) successively, a strong blue fluorescence was initially observed, but its intensity gradually decreased in the following 180 minutes, which indicated the consumption of Cys in the living cells. Correspondingly, the fluorescence emission in the green channel increased obviously, which reflected the endogenous production of sulfinate. The merged images also exhibited the concentration changes of Cys and sulfinate. These results indicated the ability to use **LC-1** to image the metabolism of Cys into SO_3^{2-} in living cells.
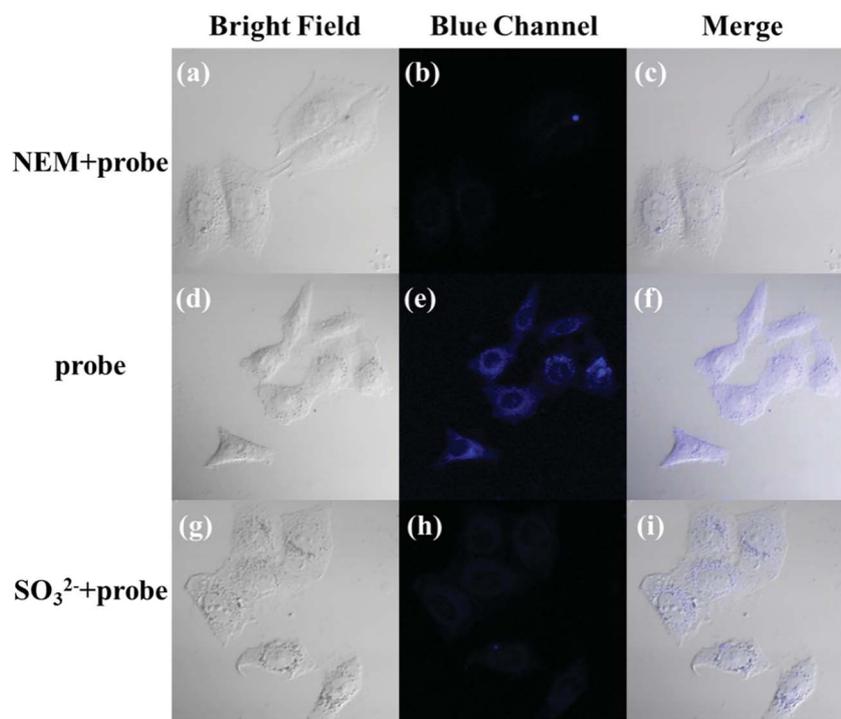

Fig. 5 Bright-field and fluorescence images of MCF-7 cells stained with the **LC-1** probe (λ_{ex} = 405 nm, λ_{em} = 430−470 nm). (a–c) Bright-field and fluorescence images of the cells incubated with N-ethylmaleimide (NEM, 2 mM) for 60 min, and then co-incubated with the **LC-1** probe for 20 min. (d–f) Bright-field and fluorescence images of cells incubated only with the probe for 20 min. (g–i) Bright-field and fluorescence images of cells incubated with Na_2SO_3 for 20 min, and then treated with the probe for 20 min.
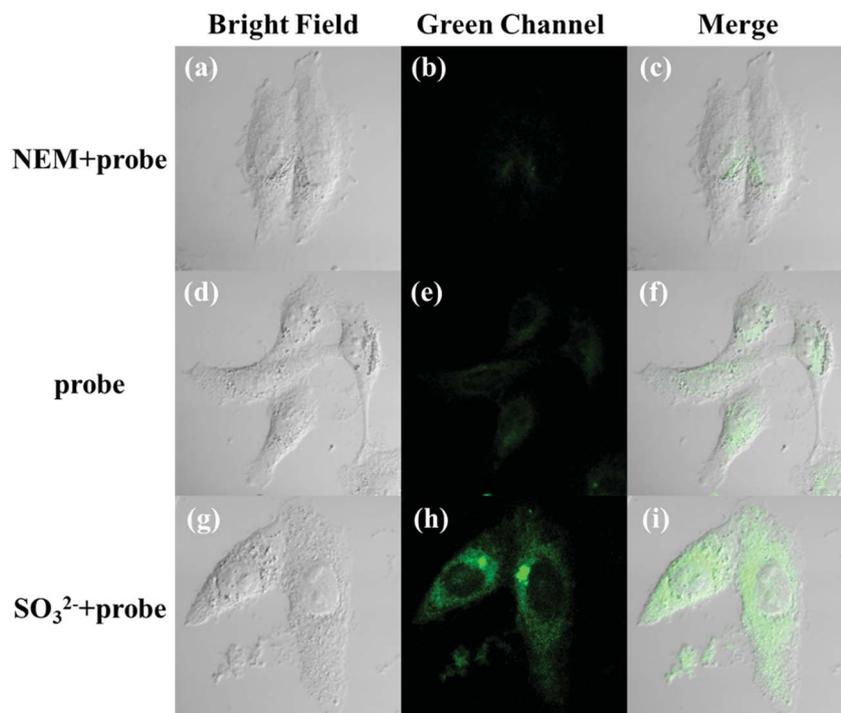
Fig. 6 Bright-field and fluorescence images of MCF-7 cells stained with the **LC-1** probe (λ_{ex} = 488 nm, λ_{em} = 490–560 nm). (a–c) Bright-field and fluorescence images of the cells incubated with N-ethylmaleimide (NEM, 2 mM) for 60 min, and then co-incubated with the **LC-1** probe for 20 min. (d–f) Bright-field and fluorescence images of cells incubated only with the probe for 20 min. (g–i) Bright-field and fluorescence images of cells incubated with Na_2SO_3 for 20 min, and then treated with the probe for 20 min.
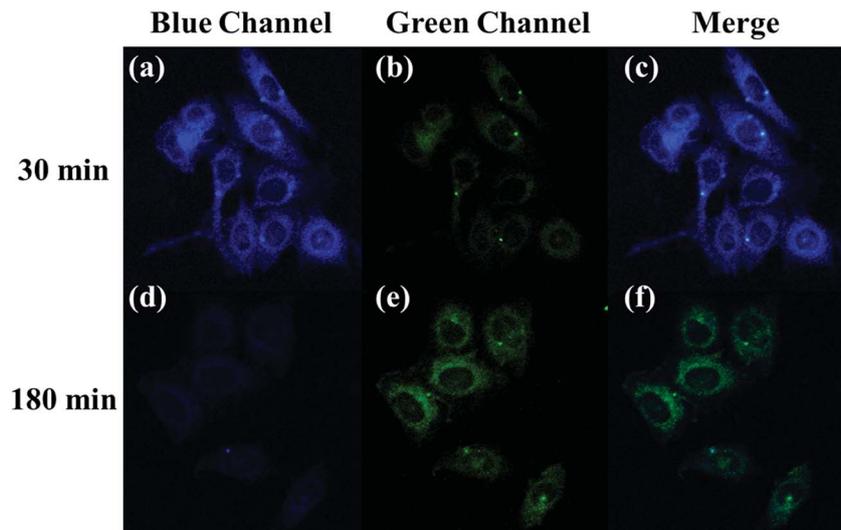

Fig. 7 Fluorescence images of MCF-7 cells incubated for two different durations with NEM, Cys, and probe successively. Blue channel: λ_{ex} = 405 nm, λ_{em} = 430–470 nm. Green channel: λ_{ex} = 488 nm, λ_{em} = 490–560 nm.

4. Conclusions

We have successfully designed and synthesized a dual-site fluorescent probe, denoted as **LC-1**, and showed it to emit different fluorescence signals through two emission channels for Cys and its metabolite SO_3^{2-}. The probe showed excellent sensitivity and selectivity for visualizing the metabolism of Cys. Experiments using cells demonstrated the satisfactory cell membrane permeability and low cytotoxicity of the probe, as well as the ability to use it to image Cys and SO_3^{2-} in living cells. We suggest that this probe may serve as an effective tool for investigations and diagnosis of Cys-associated diseases.

Conflicts of interest

There are no conflicts to declare.

Acknowledgements

References

1 F. Ali, H. A. Anila, N. Taye, R. G. Gonnade, S. Chattopadhyay and A. Das, *Chem. Commun.*, 2015, **51**, 16932–16935.

2 X. Dai, Q. H. Wu, P. C. Wang, J. Tian, Y. Xu, S. Q. Wang, J. Y. Miao and B. X. Zhao, *Biosens. Bioelectron.*, 2014, **59**, 35–39.

3 X. H. Gao, X. H. Li, L. H. Li, J. Zhou and H. M. Ma, *Chem. Commun.*, 2015, **51**, 9388–9390.

4 H. Jurkowska, L. L. Hirschberger, H. B. Roman, M. Wrobel and M. H. Stipanuk, *FASEB J.*, 2013, **27**(suppl. 1), 631.

5 W. Xu, C. L. Teoh, J. J. Peng, D. D. Su, L. Yuan and Y. T. Chang, *Biomaterials*, 2015, **56**, 1–9.

6 J. Yin, W. K. Ren, G. Yang, J. L. Duan, X. G. Huang, R. J. Fang, C. Y. Li, T. J. Li, Y. L. Yin, Y. Q. Hou, S. W. Kim and G. Y. Wu, *Mol. Nutr. Food Res.*, 2016, **60**, 134–146.

7 H. Amano, D. Kazamori, K. Itoh and Y. Kodera, *Drug Metab. Dispos.*, 2015, **43**, 749–755.

8 P. Allain, A. Lebouil, E. Cordillet, L. Lequay, H. Bagheri and J. L. Montastruc, *Neurotoxicology*, 1995, **16**, 527–529.

9 J. T. Hou, J. Yang, K. Li, K. K. Yu and X. Q. Yu, *Sens. Actuators, B*, 2015, **214**, 92–100.

10 R. R. Nawimanage, B. Prasai, S. U. Hettiarachchi and R. L. McCarley, *Anal. Chem.*, 2017, **89**, 6886–6892.

11 Y. W. Yu, J. J. Yang, X. H. Xu, Y. L. Jiang and B. X. Wang, *Sens. Actuators, B*, 2017, **251**, 902–908.

12 B. C. Zhu, L. Wu, Y. W. Wang, M. Zhang, Z. Y. Zhao, C. Y. Liu, Z. K. Wang, Q. X. Duan and P. Jia, *Sens. Actuators, B*, 2018, **259**, 797–802.

13 N. Li, J. X. Huang, Q. Q. Wang, Y. Q. Gu and P. Wang, *Sens. Actuators, B*, 2018, **254**, 411–416.

14 B. C. Zhu, L. Wu, M. Zhang, Y. W. Wang, C. Y. Liu, Z. K. Wang, Q. X. Duan and P. Jia, *Biosens. Bioelectron.*, 2018, **107**, 218–223.

15 B. C. Zhu, L. Wu, M. Zhang, Y. W. Wang, Z. Y. Zhao, Z. K. Wang, Q. X. Duan, P. Jia and C. Y. Liu, *Sens. Actuators, B*, 2018, **263**, 103–108.

16 J. X. Huang, N. Li, Q. Q. Wang, Y. Q. Gu and P. Wang, *Sens. Actuators, B*, 2017, **246**, 833–839.

17 L. W. He, X. L. Yang, K. X. Xu, X. Q. Kong and W. Y. Lin, *Chem. Sci.*, 2017, **8**, 6257–6265.

18 D. Kand, T. Saha and P. Talukdar, *Sens. Actuators, B*, 2014, **196**, 440–449.

19 X. L. Liu, L. Y. Niu, Y. Z. Chen, Y. Yang and Q. Z. Yang, *Biosens. Bioelectron.*, 2017, **90**, 403–409.

20 B. K. Rani and S. A. John, *Biosens. Bioelectron.*, 2016, **83**, 237–242.

21 J. Wang, C. Zhou, W. Liu, J. Zhang, X. Zhu, X. Liu, Q. Wang and H. Zhang, *Photochem. Photobiol. Sci.*, 2016, **15**, 1393–1399.

22 H. J. Xiang, H. P. Tham, M. D. Nguyen, S. Z. Fiona Phua, W. Q. Lim, J. G. Liu and Y. Zhao, *Chem. Commun.*, 2017, **53**, 5220–5223.

23 L. Y. Niu, Y. S. Guan, Y. Z. Chen, L. Z. Wu, C. H. Tung and Q. Z. Yang, *Chem. Commun.*, 2013, **49**, 1294–1296.

24 W. Q. Chen, Q. Fang, D. L. Yang, H. Y. Zhang, X. Z. Song and J. Foley, *Anal. Chem.*, 2015, **87**, 609–616.

25 W. Q. Chen, H. C. Luo, X. J. Liu, J. W. Foley and X. Z. Song, *Anal. Chem.*, 2016, **88**, 3638–3646.

26 X. Dai, T. Zhang, Y. Z. Liu, T. Yan, Y. Li, J. Y. Miao and B. X. Zhao, *Sens. Actuators, B*, 2015, **207**, 872–877.

27 Z. H. Fu, X. Han, Y. Shao, J. Fang, Z. H. Zhang, Y. W. Wang and Y. Peng, *Anal. Chem.*, 2017, **89**, 1937–1944.

28 X. Y. Han, F. B. Yu, X. Y. Song and L. X. Chen, *Chem. Sci.*, 2016, **7**, 5098–5107.

29 L. He, X. Yang, K. Xu and W. Lin, *Anal. Chem.*, 2017, **89**, 9567–9573.

30 W. Niu, L. Guo, Y. Li, S. Shuang, C. Dong and M. S. Wong, *Anal. Chem.*, 2016, **88**, 1908–1914.

31 P. Wang, Q. Wang, J. Huang, N. Li and Y. Gu, *Biosens. Bioelectron.*, 2017, **92**, 583–588.

32 P. Wang, Y. Wang, N. Li, J. X. Huang, Q. Q. Wang and Y. Q. Gu, *Sens. Actuators, B*, 2017, **245**, 297–304.

33 Q. Wang, H. Wang, J. Huang, N. Li, Y. Gu and P. Wang, *Sens. Actuators, B*, 2017, **253**, 400–406.

34 Y. Yue, F. Huo, P. Ning, Y. Zhang, J. Chao, X. Meng and C. Yin, *J. Am. Chem. Soc.*, 2017, **139**, 3181–3185.